

Contents lists available at ScienceDirect

Geoderma

journal homepage: www.elsevier.com/locate/geoderma



Photooxidation of pyrogenic organic matter reduces its reactive, labile C pool and the apparent soil oxidative microbial enzyme response



Ruzhen Wang ^{a,b,c}, Christy D. Gibson ^{b,c}, Timothy D. Berry ^{b,c}, Yong Jiang ^a, Jeffrey A. Bird ^d, Timothy R. Filley ^{b,c,*}

- ^a State Engineering Laboratory of Soil Nutrient Management, Institute of Applied Ecology, Chinese Academy of Sciences, Shenyang 110164, China
- ^b Department of Earth, Atmospheric, and Planetary Sciences, Purdue University, West Lafayette, IN 47907, USA
- ^c Purdue Climate Change Research Center, Purdue University, West Lafayette, IN 47907, USA
- ^d School of Earth & Environmental Sciences, Queens College, City University of New York, Flushing, NY 11367, USA

ARTICLE INFO

Article history: Received 11 August 2016 Received in revised form 23 December 2016 Accepted 5 January 2017 Available online xxxx

Keywords:
Photooxidation
Photochemical weathering
Pyrogenic organic matter
Black carbon
Oxidative enzymes
Lignin
Weathering
Priming

ABSTRACT

The surface chemistry of pyrogenic organic matter (PyOM) is altered by a variety of abiotic and biotic oxidative and sorption/desorption processes in the environment. Exposure of PyOM to high energy light prior to addition to soil or sediment, or while entrained in the atmosphere, may induce significant surface photooxidation, i.e., photochemical weathering, altering its environmental reactivity. We report on a 30-day soil incubation experiment testing the effects of the photochemical weathering of a ¹³C-enriched ponderosa pine PyOM, produced by pyrolysis at 450 °C, on PyOM and soil organic carbon (SOC) mineralization. PyOM C mineralization was measured for both the photochemically weathered (i.e. UV treated PyOM or PyOMUV) and PyOM not exposed to high-energy light (i.e. PyOMW serving as a dark control). PyOMW exhibited a 3.7 times faster C mineralization rate across the 30-d study, which was driven by a large early mineralization of accessible/labile C during the first 6 d. In contrast, PyOMUV had faster C mineralization rates in the later part of the experiment (days 11–30). Overall, PyOMUV had a 13% lower net C mineralization than the untreated PyOMW where the MRT of accessible PyOMUV-C and PyOMW-C was calculated at 25.7 ± 6.8 d and 1.7 ± 0.2 d, respectively. Both forms of PyOM promoted a similar net reduction in native SOC mineralization (i.e., negative priming) of approximately 50% relative to the unamended, control soil. Addition of either PyOM form resulted in an equivalent minor decrease in the concentration of extractable soil lignin phenols and substituted fatty acids chemistry with respect to the unamended soil. At 30 d, soil phenol oxidase and peroxidase enzyme activities were higher with additions of either form of PyOM compared with the unamended control soils with PyOMUV exhibiting lower activities than PvOMW. Our results indicate that PvOM photochemical weathering can impart important changes to short-term PyOM reactivity and soil microbial activity, which could have important implications for soil systems by ultimately lowering turnover rates for both NSC and PyOM-C.

© 2017 Elsevier B.V. All rights reserved.

1. Introduction

Pyrogenic organic matter (PyOM), a product of incomplete combustion of plant biomass or fossil fuels (Czimczik et al., 2005; Singh et al., 2012), can account for a significant proportion (5–45%) of soil carbon (C) (Glaser et al., 1998; Skjemstad et al., 2002; Hamilton and Hartnett, 2013; Santín et al., 2015), atmospheric particulate C (Bond et al., 2013; Antiñolo et al., 2015), dissolved organic C in riverine

E-mail address: filley@purdue.edu (T.R. Filley).

(Jaffé et al., 2013), estuarine and coastal waters (Mannino and Harvey, 2004), and may represent up to 65% organic C in some marine sediments (Masiello and Druffel, 1998; Middelburg et al., 1999, Cong et al., 2013). For PyOM derived from a particular biomass source, the primary control determining its resistance to environmental weathering is its temperature of production (Lehmann et al., 2015). Higher temperature exposure typically imparts physicochemical properties, primarily its highly condensed aromatic structure, that increases its stability (Skjemstad et al., 2002; Zimmerman et al., 2011; Singh et al., 2012) and resistance to biological and chemical weathering. PyOM formed under thermal conditions approximating natural forest fires, with temperature maxima ranging from ~300 to ~950 °C (Ryan, 2002; Santín et al., 2016), exhibit mean residence times (MRT) in soils from ~200 to ~600 years, which greatly exceeds that of uncharred plant materials and most non occluded particulate soil organic C (Santos et al., 2012; Singh et al., 2012, Maestrini et al., 2014).

Abbreviations: PyOM, pyrogenic organic matter; NSC, native soil carbon; SFA, substituted fatty acids; FTIR, Fourier-transform infrared spectroscopy; XPS, X-ray photo-electron spectroscopy.

^{*} Corresponding author at: Department of Earth, Atmospheric, and Planetary Sciences, Purdue University, West Lafayette, IN 14907, USA.

Specific plant taxa may vary in the temperature at which important thermally-driven physicochemical transitions occur during pyrolysis (Hatton et al. 2016). Over a given temperature range, significant chemical (e.g., aromatization of lignocellulose, loss of waxes) and ultrastructural (e.g., increases in specific surface area, shrinking cell volume) changes occur (Keiluweit et al., 2010; Hatton et al., 2016), imparting different degrees of thermodynamic and kinetic influence on PyOM environmental reactivity (Zimmerman, 2010; Zimmerman et al., 2011). The ever-growing research focus on PyOM has demonstrated how complex interactions within soil control the mechanisms and rates of degradation PyOM (Brodowski et al., 2005; Schmidt et al. 2001; Singh et al., 2012; Maestrini et al., 2014, 2015).

Apart from the thermally-driven changes to biomass occurring during pyrolysis, the physicochemical properties of the surface of PyOM particles can be altered by biotic and abiotic oxidative processes in the environment including exposure to UV radiation in the atmosphere (Antiñolo et al., 2015) or on the soil surface (Cheng et al., 2008), and microbial-driven processes in soils (LeCroy et al., 2013; Wang et al., 2016). This has important implications for PyOM fate as the pyrolysis conditions of high thermal exposure (>400 °C), forest and grass fires remove most reactive oxygen containing functional groups from PyOM (Almendros et al., 1992; Liu et al., 2013). As a result, oxidative weathering pathways, through photolytic or microbial oxidation for example, are needed to reintroduce reactive functional groups that could increase PyOM environmental weathering through enhanced solubility, surface binding capacity, or microbial enzyme induction effects (Wang et al., 2016; Gibson et al., 2016). Controlled degradation experiments of other highly condensed aromatic particles and compounds (e.g. manufactured nanocarbon such fullerols, fullerenes, and carbon nanotubes) that have structural and chemical similarities to graphitic phases within high temperature PyOM suggest that surface functionalization (e.g., hydroxylation or carboxylation) enhances the enzymatic response of soil microorganisms toward degradation such structures (Berry et al., 2014, 2016a,b; Schreiner et al., 2009).

Natural or intentional (i.e., through agricultural biochar amendments) additions of PyOM to soil can affect the rate of mineralization of the original (native) soil carbon (NSC) resulting in either an increase (i.e., positive priming), a decrease (negative priming), or stasis in the net NSC converted to CO₂ (Kuzyakov et al., 2009, 2014; Maestrini et al., 2015). Positive priming effects are linked to the proliferation or increased activity of soil microbes, induced by a variety changes including nutrient accessibility (Laird et al., 2010; Yao et al., 2012; Prendergast-Miller et al., 2014), pH (Jain et al., 2016; Jin et al., 2016), and creation of favorable microenvironments (Lehmann et al., 2011). Co-metabolism of labile PyOM and NSC is a widely suggested mechanism for observations of positive priming within the first few days of mixing into nutrient limited soils (Bruun et al., 2011; Luo et al., 2011; Lin et al., 2015; Murray et al., 2015). Furthermore, the addition of the aromatic PyOM C is thought to stimulate the production of microbial extra-cellular oxidative enzymes leading to increases in the decomposition of C pools proximal to the PyOM (Zimmerman et al., 2011; Thies et al., 2015; Gibson et al., 2016). Suggested mechanisms for negative priming effects have included the physical protection of soluble NSC on PyOM surfaces or within its pores (Smernik and Skjemstad, 2008; Kasozi et al., 2010), binding and blocking of extracellular microbial enzyme active sites (Lammirato et al., 2011), or the suppressive activity of antimicrobial compounds leached from the PyOM (Lehmann et al., 2011; Kim et al., 2012). As the proposed controls on priming should be significantly influenced by PyOM surface chemistry, environmental oxidation of PyOM could be an important factor for determining the response of NSC to PyOM addition.

In a recent study investigating the interaction of a saprotrophic white-rot fungus with a ponderosa pine-derived PyOM produced by fast pyrolysis at 450 °C we (Gibson et al., 2016) demonstrated that photochemical (UV) weathering of the PyOM induced a distinct enzymatic response in the fungus as compared to the unphotolyzed PyOM. While

the fungus, Trametes versicolor, did not significantly mineralize PyOM-C in either treatment, both forms of PyOM caused an increase in mineralization of the culture growth media. The photochemically- weathered PyOM also resulted in a suppressed enzyme response by the fungus and lower degree of media mineralization. These observed changes were speculated to be the direct result of weathering-induced surficial chemistry as the UV treated PyOM exhibited higher surface oxygen content (as determined by FTIR and XPS) and a relative decrease in aromatic C to aliphatic C-H surface signatures (as determined by FTIR). Gibson et al. (2016) proposed that the fungal enzyme system alone might be insufficient to oxidize the complex aromatic structure of weathered PyOM and that a complex microbial consortium such as that present in soil was needed for mineralization. These results were consistent with Boonchan et al. (2000) who demonstrated that significant degradation of high molecular-weight polycyclic aromatic hydrocarbons only occurred in combined fungal-bacterial cultures but not axenic cultures, highlighting the importance of complex microbial systems with numerous synergistic degradative processes (Bouchez et al., 1999; Boonchan et al., 2000; Peng et al., 2008). Additionally, a recent field and related lab study investigating the decay of ¹³C-labeled PyOM demonstrated that while the broad microbial community is capable of taking up PyOM carbon, fungi showed lower anabolic use of PyOM-C compared to bacteria (Santos et al., 2012).

Herein we report on a 30-day soil incubation experiment testing the effects of PyOM photochemical weathering on PyOM dynamics in soil using the same 13C-enriched Pinus ponderosa wood PyOM used in Gibson et al. (2016). We compare PyOM C and NSC mineralization using stable carbon isotope monitoring of mineralized CO2 and the apparent activities of soil phenol oxidase and peroxidase among incubations amended with PyOM either UV reacted while in a water slurry (PyOMUV), or in the absence of light as a dark control (PyOMW). In Gibson et al. (2016), we postulated that labile components on the PyOMUV surface were photochemically degraded prior to exposure to the fungi which corresponded to the observed differences in reactivity. The same hypothesis guides our speculation in the current study. We predict that: (1) C mineralization of the photochemically weathered PyOMUV will occur at a slower rate than the dark control (PyOMW) due to relatively lower concentration and accessibility of labile C to soil microbes in PyOMUV; (2) addition of PyOMUV to soil will result in lower apparent oxidative enzyme activity than in PyOMW treatments, however both PyOM treatments should increase apparent soil enzyme activities relative to the un-amended control soil; and (3) the magnitude of the induced NSC priming effects on fast and slow turnover NSC pools, evidenced by bulk soil mineralization as well as with changes in soil lignin phenol and substituted fatty acid content should be less with the addition of PyOMUV relative to the PyOMW treatments.

2. Materials and methods

2.1. Production of PyOM and analysis of its properties

Detailed description of ponderosa pine (*Pinus ponderosa*) sapling growth under ¹³C-CO₂ atmosphere can be found in Bird and Torn (2006). Stems harvested from the saplings were pyrolized at a constant 450 °C for 5 h under N₂ according to procedures in Hammes et al. (2006). The resulting PyOM was then ground to a particle size <2 mm. ¹³C solid-state NMR, Fourier transform infrared spectroscopy, elemental analysis, benzene polycarboxylic acids (BPCAs) composition and stable isotope analysis were performed to determine bulk and surface characteristics, ¹³C isotopic signature, and to confirm the uniformity of the isotopic label of the initial charred material (Yarnes et al., 2011, Chatterjee et al., 2012). The overall isotopic composition of the PyOM was 848‰ (2.3 atom% ¹³C) expressed with respect to international standard Vienna PeeDee Belemnite (V-PDB). The elemental abundance of %C, %H and %O was, 77.9%, 3.4% and 14.4%, respectively (Santos et al., 2012).

2.2. Photochemical weathering of PvOM and analysis of surface chemistry

Weathering effects by UV light were simulated by reacting the PyOM in a deionized water slurry for 4 weeks under UV (254 nm) light (PyOMUV) exposure according to procedures outlined in Gibson et al. (2016). PyOM mixed in the same water slurry but shielded from light (denoted as PyOMW) was set as a dark control for this artificial photochemical weathering experiment. Briefly, subsamples of 30 mg ¹³C-PyOM were loaded into eight 16 ml quartz vials (New England Ultraviolet Company, Branford, CT) and mixed with 10 ml ultra-pure water. Vials were sealed and attached to a gently rotating carousel (5 rpm). Treatments included vials exposed to two UV (PyOMUV) light lamps and vials shielded from light (PyOMW) by being wrapped in aluminum foil. The intensity of UV light was $\sim 1.5 \times 10^{-9}$ Einstein cm²/s resulting in a cumulative energy exposure of ~1879 W/cm² over four weeks (Gibson et al., 2016). This amount of energy is roughly equivalent to 11 d of solar radiance at mid latitudes (39°16′22″N) at 2944 m above sea level (McKenna and Andreas, 1997). The PyOMUV and PyOMW samples were recovered by filtering the slurry through a 0.22 µm cellulose acetate filter and then air-drying in the dark. Production of PyOMUV resulted in ¹³CO₂ evolution indicating UV-induced oxidation while PyOMW showed no ¹³CO₂ production (Gibson et al., 2016). The surface chemistry of both PyOMW and PyOMUV samples was assessed by Fouriertransform infrared spectroscopy (FTIR) and X-ray photoelectron spectroscopy (XPS). Results were presented in previous work (Gibson et al., 2016). Briefly, PyOMUV exhibited increased surface oxygen, loss of aromatic C—H, higher contribution of the carbonyl to carboxylate bands, and increased aliphatic C—H stretching with respect to PyOMW.

2.3. Soil incubation experiment

Soil (0–5 cm depth) was collected in 2012 from within an ongoing fire manipulation experiment at the University of Michigan Biological Station (Pellston, MI, USA; 45°35′N, 84°43′W). The area of sampling was last burned in 1980 and soils (0-5 cm) used in the incubation were collected from four 25-m long transects, combined, sieved to 2 mm to remove plant litter and stones, air dried (~22 °C) and stored until use. The soil is described as well drained, sandy, mixed frigid Entic Haplorthods of the Rubicon series and is ~92% sand, ~7% silt, and ~1% clay with an estimated PyOM C content of ~0.58-9 µg C g⁻¹ soil (Yarnes et al., 2011). The bulk soil pH was 5.2 \pm 0.3 according to Lierop (1990). Dry soil was subsampled and ground for elemental and stable isotope measurement using a Sercon Ltd. (Crewe, U.K.) GSL elemental analyzer interfaced to a Sercon Ltd. 20–22 Isotope Ratio Mass Spectrometer (IRMS). Elemental and stable isotope analysis showed the bulk soil to be 1.79% \pm 0.28C and 0.07% \pm 0.01 N by mass with a δ^{13} C value of $-27.5\% \pm 0.2$. Previous size and density separation of the soils (0-5 cm) from this site demonstrated that more than half of the soil C resides in particulate organic carbon (POC) not associated with mineral surfaces with only ~37% of soil C strongly associated with mineral surfaces (McFarlane et al., 2012).

To construct the incubation vessels, sterilized glass wool was packed into 12 ml, autoclaved Labco Exetainer vials (Labco Ltd., Ceredigion, UK) in order to prevent caking of soils and the development of anaerobic zones. Then 3 g of soil was added to each vial and rewetted to 55% water holding capacity (WHC) by adding 0.9 ml autoclaved deionized water. The soils were then pre-incubated for 5 d before the addition of PyOMW or PyOMUV. PyOM-C was added to soil at a loading rate of 10% (~5.5 mg per vial) of original (native) soil C and gently mixed. Incubation of unamended soil served as an absolute control and was treated identically as those that received added PyOM. Five analytical replicate vials were used per treatment. Vials were capped with glass fiber filter to permit air exchange when not accumulating gases before being placed into a temperature controlled room in the dark at 25 °C and incubated for 30 d.

2.4. Headspace ¹³CO₂ determination and modeling

To distinguish between mineralization of NSC and 13 C-labeled PyOM-C, headspace CO $_2$ concentration and 13 C enrichment were determined with a Sercon Ltd. (Crewe, U.K.) Cryoprep Trace Gas Analyzer (TG2) interfaced to a Sercon 20–22 Isotope Ratio Mass Spectrometer (IRMS). CO $_2$ measurements were conducted at days 1, 2, 6, 11, 16, 24, and 30 after PyOM amendment by automated flushing of the microcosm headspace. Prior to headspace accumulation, glass fiber filters on each vial were replaced by gas-tight, reusable rubber septa. Vials were then flushed with 10 times their volume using humidified CO $_2$ -free air. The water content of each microcosm was checked by weighing each vial weekly. On day 24, approximately 0.1 ml of water was added to each vial to replace lost water. The fraction of evolved C from PyOM (f_{PyOM}) and from NSC (f_{NSC}) was calculated using a two-component isotopic mixing model:

$$f_{\text{PyOM}}(\%) = \frac{\delta^{13}\text{CO}_{2\text{-measured}} - \delta^{13}\text{CO}_{2\text{-NSC}}}{\delta^{13}\text{C}_{\text{PyOM}} - \delta^{13}\text{CO}_{2\text{-NSC}}} \times 100 \tag{1}$$

where $\delta^{13}\text{CO}_{2\text{-measured}}$ is the $\delta^{13}\text{C}$ value of total CO₂-C evolved from soil-PyOM mixtures, $\delta^{13}\text{CO}_{2\text{-NSC}}$ is the $\delta^{13}\text{C}$ value for the CO₂-C evolved from control soil (no PyOM addition), and $\delta^{13}\text{C}_{\text{PyOM}}$ is the ^{13}C isotopic composition of PyOM.

NSC mineralization rates for days 1–16 were modeled as containing two conceptual carbon pools characterized by fast and slow turnover by applying the following double exponential decay model (Paul et al., 2001; Creamer et al., 2011):

$$-dC/dt = C_F e^{-k_F t} + C_S e^{-k_S t}$$
 (2)

where dC/dt is in units of mg C day⁻¹, C_F and C_S are the fast and slow turnover pools respectively and k_F and k_S are the rate constants for the fast and slow turnover pools. The total size of these pools was calculated by integrating the first order differential equation describing each pool:

$$C_{Ti} = C_i / -k_i \Big(e^{k_{i \, t}} - 1 \Big) \eqno(3)$$

NSC respiration rates for day 24 and 30, following the second water addition, were treated as a discrete linear interval and the amount of this C-pool liberated after rewetting (referred to hereafter as C_{SP}) was estimated with following equation:

$$Csp = (t_2 - t_1) \left[\frac{R(t_1) + R(t_2)}{2} \right] \tag{4} \label{eq:4}$$

where (t_2-t_1) is the time increment between days 30 and 24, respectively, of the incubation and R represents rate of respiration at t_2 and t_1 . Fluctuation in PyOM-C mineralization rates did not follow a specific

function. As a result, the cumulative percent of total PyOM-C (PyOMW or PyOMUV) respired at time t (C_{PyOM-t}) was calculated as:

$$C_{PvOM-t} = \sum_{i=1}^{n} (R_t \times T_t) \tag{5}$$

where C_{PyOM-t} is the cumulative percent total PyOM-C respired at time t; n is the number of total time points in this experiment, R_t is mineralization rate of time t, T_t is the time elapsed between time (t-1) and t. This value for each discrete time interval was then subtracted from the initial amendment mass of PyOM-C to calculate PyOM-C remaining. The MRT of the fast cycling C pool was then calculated by applying a double exponential model as with NSC (Eq. (2)). The resulting rate constant (k_f) was

used to calculate the mean residence time as follows:

$$MRT_f = 1/k_{(f)} \tag{6}$$

The priming effect of PyOM on NSC at time t was determined as follows:

$$PE_{t} = R_{treatment-t} - R_{control-t}$$
 (7)

where $R_{control-t}$ and $R_{treatment-t}$ are the rate of NSC mineralized in the control soil without PyOM addition and soil with PyOM addition, respectively, at the time point t.

2.5. Enzyme assays

The potential activities of extracellular phenol oxidase and peroxidase soil-bound enzymes were quantified at the termination of the incubation using a colorimetric assay measuring the oxidation of the substrate L-3,4-dihydroxyphenylalanine (L-DOPA) as described by Weintraub et al. (2007). Briefly, 1 g of moist soil collected after the incubation experiment from each treatment and control replicate (n = 5)was added individually into 50 ml of 50 mM sodium acetate buffered at a pH of 5, similar to the pH of the bulk soil (5.2 \pm 0.3) and placed on a stir plate in the dark for 1 h. 10 ml of soil extract was mixed with 10 ml of 25 mM L-DOPA and incubated at 25 °C for 24 h. Duplicate soil extracts + L-DOPA, as well as 625 μl of 0.3% H₂O₂, were prepared to assay for peroxidase activity. The incubated reaction solutions were centrifuged to settle out particles that may have interfered with UV light absorption measurements and transferred to acrylic cuvettes for analysis. Activity was measured by UV-VIS spectroscopy at a wavelength of 460 nm.

2.6. Lignin and substituted fatty acid extraction and quantification

To determine the differential decomposition effects of PyOM amendments at the biopolymer level, plant derived soil lignin and substituted fatty acids (SFAs), plant components of purportedly lower reactivity than the bulk soil, were extracted with the alkaline cupricoxide (CuO) oxidation technique following procedures from Hedges et al. (1982) and Goñi and Hedges (1990) with modifications outlined in Filley et al. (2008). The trimethylsilyl (TMS) derivatives of vanillyl (V)-based (i.e., vanillin, acetosyringone, vanillic acid), syringyl (S)based (i.e., syringaldehyde, acetosyringone, syringic acid), and cinnamyl (Ci)-based (i.e., p-hydroxycinnamic acid and ferulic acid) lignin were quantified via GC/MS (Filley et al., 2008) and the total yield of lignin phenols was denoted as 'SVCi-lignin'. The TMS derivatives of SFAs were determined by summing the masses of eight monomers including 16-hydroxyhexadecanoic (ω-C₁₆), hexadecane-1,16-dioic $(C_{16}DA)$, 18-hydroxyoctadec-9-enoic $(\omega - C_{18:1})$, 9,16&10,16-dihydroxyhexadecanoic (9&10, ω -C₁₆), 9-octadecene-1,18-dioic (C_{18:1}DA), 7&8hydroxyhexadecane-1,16-dioic (7&8-C₁₆DA), 9,10,18-trihydroxyoctadec-12enoic (9,10, ω-C_{18:1}), and 9,10,18-trihydroxyoctadecanoic $(9,10, \omega$ -C₁₈). Compound concentrations are given as mg compound/ 100 mg NSC. The lignin phenol ratios Ci/V, S/V were investigated to assess changes in individual lignin content due to selective decomposition while lignin oxidization was assessed through the relative concentration ratios of vanillic to vanillin, Ad/Al(V), and syringic to syringaldehyde, Ad/Al(S) (Hedges and Ertel 1982).

2.7. Statistical analyses

The normality of data was tested by using the Kolmogorov-Smirnov test and homogeneity of variances was determined by Levene's test. Completely randomized one-way ANOVA was used to test if PyOM additions significantly affected phenol oxidase and peroxidase activities,

SVCi-lignin and SFAs concentrations, or the ratios of Ci/V, S/V, Ad/Al(V) and Ad/Al(S). Repeated-measures ANOVA was used to test the treatment effects on $\delta^{13}CO_2$, soil total CO_2 respiration rates, cumulative PyOM-C and NSC respired, and priming effects of added PyOM. For each time point, a Tukey's post-hoc analysis was conducted to determine significant differences in $\delta^{13}C$, cumulative NSC mineralized and priming effect of PyOM on NSC among the PyOMUV, PyOM and control treatments. All the statistical analyses were performed in SPSS 16.0 (SPSS, Inc., Chicago, IL, U.S.A.) with $\alpha < 0.05$.

3. Results

3.1. Native soil C (NSC) and PyOM mineralization

At all time-points, except sampling day 16, NSC mineralization rates were lower for soils containing PyOMW and PyOMUV (P < 0.01) when compared to unamended soil controls (Table 1). Overall, mean NSC mineralization rates decreased by 37.0% and 43.0% for PyOMUV and PyOMW, respectively, however there were no significant differences in NSC mineralization rates between PyOMW and PyOMUV treatments. Water addition on day 24 resulted in an increase in the NSC mineralization rates for all treatments with unamended control increasing by 517% and PyOMUV and PyOMW increasing to lesser degrees at 69% and 135% from day 16. The largest suppressive effect on NSC mineralization by PyOM addition was seen on day 24.

PyOMUV-C mineralization rates ranged from 1.7 to 61.3 μg CO₂-C g⁻¹ PyOMUV-C day⁻¹ during the 30-d incubation while PyOMW mineralization rates exhibited a higher range at 3.3 to 606.2 μg CO₂-C g⁻¹ PyOMW-C day⁻¹ (Table 2). The rates of $^{13}\text{CO}_2$ production from the two PyOM treatments varied throughout the course of the experiment with PyOMW exhibiting higher rates than PyOMUV on days 1 and 6 but dropping to relatively lower values on days 11, 16, and 24. Net PyOMW mineralization was 14% higher than the photochemically weathered PyOMUV resulting in estimated mean residence times of 1.7 d vs 25.7 d respectively, for the fast cycling PyOM C pool (Table 3). This difference was largely driven by the much lower PyOMUV C mineralization rates compared to PyOMW on day one (11.8 vs 606 μg CO₂-C g⁻¹ PyOM-C day⁻¹, respectively).

3.2. NSC priming effects and modeled C pools

A net negative priming effect (PE) was exhibited for both PyOMW and PyOMUV additions, with no significant difference between the PyOM forms (Table 3), where PE ranged from 0.16 ± 0.08 to -5.29 ± 0.14 mg CO₂-C g $^{-1}$ soil C day $^{-1}$ and from -0.14 ± 0.16 to -5.07 ± 0.09 mg CO₂-C g $^{-1}$ soil C day $^{-1}$ for PyOMUV and PyOMW treatments, respectively (Fig. 1). The PE trended from initially negative to near neutral prior to rewetting on day 24. The largest negative priming effect, approximately a mean value of -5.18 for both treatments, was observed after the addition of water on day 24, which then increased to -2.0 by day 30 (Fig. 1).

Addition of both the photochemically weathered and dark, control PyOMW to soil resulted in a significant reduction in the size of the NSC C_f , C_s , and C_{sp} mineralized pools with respect to the no amendment control but there were no significant differences between PyOM treatments (Fig. 2). Specifically, C_f , C_s , and C_{sp} mineralized pools decreased by an average of $80.6 \pm 0.8\%$, $52.2 \pm 6.2\%$, and $60.4 \pm 0.6\%$, respectively (Fig. 2). As observed for the net PE, PyOMUV and PyOMW had the same effects for the modeled conceptual C pool mineralization rates and over the course of the experiment (Fig. 2; Table 1), with an overall decrease of $60.9 \pm 2.9\%$ in net NSC mineralization.

3.3. Phenol oxidase and peroxidase activities

At the termination of the experiment, soil phenol oxidase enzyme activity and peroxidase activity increased with addition of both

Table 1 Soil respiration rates (mg CO₂-C g $^{-1}$ soil C day $^{-1}$) of native soil C (NSC) from 30 d incubations of unamended soil and soil amended with either photochemically weathered pyrogenic organic matter (PyOMUV) or control PyOM (PyOMW) treatments. Photochemical weathering was simulated by mixing PyOM for 4 weeks in a water slurry while exposed to UV-light (PyOMUV) and compared to PyOM mixed in a water slurry shielded from light as a dark control. Values are means \pm standard errors, n = 5. Different letters indicate significant differences among treatments for each sampling point ($\alpha = 0.05$).

Treatment	Day 1	Day 2	Day 6	Day 11	Day 16	Day 24	Day 30
Unamended soil Soil + PyOMUV	$3.4 \pm 0.1a$ $1.7 \pm 0.2b$	2.9 ± 0.2a 1.9 + 0.5a	2.5 ± 0.2a 1.1 + 0.1b	2.0 ± 0.2a 1.4 + 0.1b	1.2 ± 0.1 a $1.4+0.1$ a	$7.7 \pm 0.6a$ 2.4 + 0.1b	$3.9 \pm 0.2a$ 2.1 + 0.1b
Soil + PyOMW	$1.5 \pm 0.1b$	$1.8 \pm 0.4a$	$1.2 \pm 0.1b$	$1.3 \pm 0.1b$	$1.1 \pm 0.2a$	$2.6 \pm 0.1b$	$2.0 \pm 0.1b$

PyOMW and PyOMUV, by up to 200% for phenol oxidase, with respect to the unamended control soils (Table 4). Photochemical weathering of PyOM, however, resulted in a significantly ($\alpha=0.05$) lower (\sim 10%) apparent soil microbial enzyme activity compared to the soil with PyOMW addition. Specifically, addition of PyOMW resulted in an increase in phenol oxidase activity from 15.1 to 30.4 μ mol g $^{-1}$ soil C compared to the unamended control. Additionally, of PyOMUV treatments resulted in an activity of 26.6 μ mol g $^{-1}$ soil C with respect to unamended controls. Similarly, PyOMW and PyOMUV resulted in an increase in peroxidase activity, but with more modest changes, increasing activity from the unamended soil values of 57.9 to 66.3 and 60.6 μ mol g $^{-1}$ soil C, respectively.

3.4. Biopolymer characteristics in soils

After 30 d of incubation, extracted SVCi-lignin concentrations exhibited a slight, albeit non-significant, increase in the un-amended soil and a slight decrease in both PyOM amended treatments as compared with the initial soil. These small bifurcating effects resulted in a statistically significant (P=0.03) difference between the unamended control (2.0 mg SVCi lignin/100 mg OC) and the two PyOM treatments (~1.8 mg SVCi lignin/100 mg OC) (Fig. S1a). SFA concentrations in the PyOM exhibited a small but significant increase from the preincubated soil (Fig. S1a; P < 0.05).

The ratio of cinnamyl to vanillyl phenols (Ci/V) was not significantly changed with PyOM addition compared to the un-amended soil after 30 d (Fig. S1b). The ratio of syringyl to vanillyl phenols (S/V) exhibited a small but significant decrease for the un-amended and added PyOM as compared with the pre-incubation soil. The Ad/Al $_{\rm (N)}$ values were statistically similar among all treatments while the Ad/Al $_{\rm (S)}$ increased from 0.36 in the pre-incubated soil to 0.41 in the un-amended soil and soil with added PyOM after 30 d (Fig. S1c).

4. Discussion

4.1. Photochemical weathering affects PyOM C mineralization in soil

Informed by our previous FTIR and XPS analysis in Gibson et al. (2016) which showed that photochemical weathering oxidized the surface of PyOM, we posited in this study that there would be a distinct difference in mineralization rates of labile C content between PyOMW and its weathered analog, PyOMUV, in soil evidenced by lower C mineralization of PyOMUV. As predicted, PyOMUV exhibited a lower net mineralization (Table 2) however, the controls imparted by weathering were complex and evolved over the 30 d in that the significant mineralization observed early in the incubation (day 1–6) for PyOMW was absent for

PyOMUV but by day 11, PyOMUV mineralization rate increased and exceeded PyOMW. Overall, the MRT of PyOMUV-C and PyOMW-C during this 30 day lab study was 25.7 ± 6.8 and 1.7 ± 0.2 d respectively (Table 3) indicative of a less accessible and depleted fast cycling pool. Other studies have observed a large pulse of PyOM-C mineralized soon after addition to soils corresponding to decomposition of the initial labile C pool; further mineralization occurs at slower rates mediated by chemical, physical and biological processes (Hockaday et al., 2006; Cheng et al., 2008; Wang et al., 2016). The initial, enhanced mineralization of PyOMW compared with PyOMUV is consistent with mineralization of labile constituents on the PyOMW surface (Bruun et al., 2011; Liu et al., 2013).

After day 6 of the incubation when much of the readily accessible and labile PyOMW-C had been consumed, PyOMUV exhibited progressively greater C mineralization rates compared to PyOMW which could be a result of greater density of hydrophilic functional groups on PyOMUV, consistent with the observed oxygenated surface (Gibson et al., 2016), allowing greater accessibility of extracellular enzymes and diffusion of dissolved PyOM at the surface. Greater carboxyl and hydroxyl functional group density could allow for greater nutrient retention at the surface and potentially promote greater microbial activity (Glaser et al., 2001). The observed increase in mineralization for PyOMUV later in the incubation is consistent with other studies which postulate that weathered and more hydrophilic PyOM can be more vulnerable to microbial degradation in the longer term (Cheng et al., 2006; Nguyen et al., 2009; Zimmerman, 2010). The role of a hydrophilic surfaces promoting enhanced PyOM mineralization once labile carbon is consumed may be evident in our results after rewetting on day 24 which showed both PyOM forms increase in mineralization rate but with PyOMUV maintaining the higher overall rate at 61.3 vs. 36.3 µg CO_2 -C g^{-1} PyOM-C day⁻¹.

4.2. Photochemical weathering of PyOM does not change net NSC priming effect

Overall, both PyOMUV and PyOMW induced a negative priming effect of similar magnitude on NSC mineralization (Fig. 1). This was in contrast to our expectations based upon our previous single culture fungus decay experiment (Gibson et al., 2016) where both PyOMW and PyOMUV treatments promoted a net increase in mineralization of culture growth media C relative to the no amendment control. Previous soil amendment studies using this same ponderosa pine-sourced PyOM, albeit without the photochemical weathering treatment, showed seemingly contrasting results with both neutral (Santos et al., 2012) and positive priming effects (Singh and Cowie, 2014) on NSC mineralization. These variable results, particularly comparing PyOMW to the earlier

Table 2
PyOM C mineralized (μ g CO₂-C g⁻¹ PyOM-C day⁻¹) from 30 d soil incubations amended with either photochemically weathered pyrogenic organic matter (PyOMUV) or control PyOM (PyOMW) treatments. Photochemical weathering was simulated by mixing PyOM for 4 weeks in a water slurry while exposed to UV-light (PyOMUV) and compared to PyOM mixed in a water slurry shielded from light as a dark control. Values represent means \pm standard errors, n = 5. Different letters indicate significant differences among treatment for each sampling point ($\alpha = 0.05$).

Treatment	Day 1	Day 2	Day 6	Day 11	Day 16	Day 24	Day 30
PyOMUV PyOMW	$11.8 \pm 8.9b$ $606.2 \pm 55.2a$	31.6 ± 11.2 a 43.2 ± 9.7 a	1.7 ± 1.7 a 18.9 ± 10.5 a	$27.8 \pm 5.2a$ $3.3 \pm 2.2b$	$37.1 \pm 3.8a$ $11.2 \pm 3.0b$	$61.3 \pm 6.8a$ $36.3 \pm 8.2b$	$23.5 \pm 9.0a$ $8.0 \pm 4.0a$

Table 3 Net treatment effects of 30 d incubations of unamended soil and soil amended with either photochemically weathered pyrogenic organic matter (PyOMUV) or control PyOM (PyOMW) treatments. Compared are native soil carbon (NSC) mineralization rates (mg CO_2 –C g $^{-1}$ soil–C day $^{-1}$), PyOM C mineralization rates ($\mu^{13}CO_2$ –C g $^{-1}$ PyOM-C day $^{-1}$), priming effects of PyOM on NSC mineralization (mg $^{13}CO_2$ – $^{13}CO_2$

Treatment	NSC mineralization rates (mg CO ₂ -C g ⁻¹ soil-C day ⁻¹)	PyOM-C mineralized rates ($\mu g^{13}CO_2$ -C g^{-1} PyOM-C day ⁻¹)	Priming effect (mg CO ₂ -C g ⁻¹ soil-C day ⁻¹)	net PyOM-C mineralized (μg $^{13}CO_2$ -C g^{-1} PyOM-C)	MRT_f
Unamended soil	$3.4 \pm 0.3a$				
Soil + PyOMUV	$1.6 \pm 0.1b$	$27.8 \pm 3.9b$	-1.75 ± 0.26 a	1.01 ± 0.15a	25.7 ± 6.8a
Soil + PyOMW	$1.7 \pm 0.1b$	103.9 ± 36.0a	$-1.66 \pm 0.29a$	1.14 ± 0.09 a	1.7 ± 0.2b

Santos et al. and Singh et al. work, are most likely governed by the significant differences among the soils that were amended. Soils in the three studies ranged largely in parent material, SOC stock, and physical distribution of SOC among soil mineral and particulate fractions. Moreover, the studies differed in incubation duration and pre-incubation conditions, which also could result in contrasting priming effects (Lehmann et al., 2015). The pre-treatment of the PyOMW in a dark aqueous slurry could have also increased the capacity for surface binding of organic matter, above the "as produced" PyOM used in the previous work, thereby lowering effective concentrations of key regulatory compounds (Masiello et al., 2013) as well as native dissolved organic matter (Zimmerman et al., 2011).

In a complex medium such as soil, PyOM surface functionalization can play an important mechanistic role in the binding or complexation of dissolved soil components rendering both PyOM and the sorbed material more resistant to mineralization (Kasozi et al., 2010; Liu et al., 2013). Changes in surface activity have been shown to increase with PyOM oxidation or aging (LeCroy et al., 2013) and Liu et al. (2013) suggested that nitrobenzene adsorption increased with increasing surface oxidation of a straw, oak and bamboo-derived PyOM. In the present study, evidence for the role of surface binding can be seen in the dramatic reduction in NSC mineralization rates of both PyOM treatments compared to controls after the rewetting on day 24 (Fig. 1; Table 3). It is not surprising that the control soil incubations exhibited a large increase in CO₂ efflux upon rewetting given that rewetting soils is known to enhance respiration through release of accumulated labile C

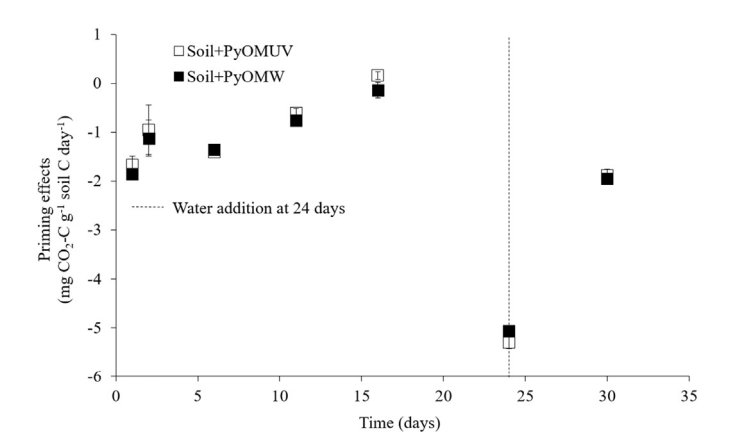


Fig. 1. Native soil C (NSC) priming effects (mg CO_2 –C g^{-1} soil C day $^{-1}$) calculated for soils amended with either photochemically weathered pyrogenic organic matter (PyOMUV) or control PyOM (PyOMW). Photochemical weathering was simulated by mixing PyOM for 4 weeks in a water slurry while exposed to UV-light (PyOMUV) and compared to PyOM mixed in a water slurry shielded from light as a dark control. Data represent means \pm standard error, n=5.

and nutrients (Fierer and Schimel, 2002; Mikha et al., 2005; Borken and Matzner, 2009; Navarro-García et al., 2012). Contrary to expectations for PyOMUV treatments, the change in PE to negative values upon rewetting was as large as $-5.5~{\rm mg~CO_2\text{--C~g}^{-1}}$ soil C day $^{-1}$. Similarly for PyOMW, the magnitude of negative PE decreased to $-4.9~{\rm mg~CO_2\text{--C~g}^{-1}}$ soil C day $^{-1}$ (Fig. 1). This shift strongly suggests that both PyOM treatments immobilized NSC onto their surface making it inaccessible. However, the highly functionalized PyOMUV immobilized labile NSC to a greater extent than PyOMW. Although microbial biomass was not quantified, a portion of the large shift to negative PE might be attributed to selective uptake of NSC into microbial biomass in the PyOM treatments, rather than conversion to CO2. Such was speculated in a recent PyOM incubation study investigating response to wetting (Wang et al., 2016).

We investigated the priming effect at the biopolymer level through extraction of lignin and substituted fatty acids. The SVCi-lignin concentration in soils with either PyOM addition was slightly, but significantly, lower than either the incubated unamended control soil or the initial soil prior to incubation (Fig. S1) indicating that only minor decay occurred during the short incubation study. Selective decomposition of soil lignin in the presence of PyOM would also be consistent with the observed increase in oxidative enzyme activity herein (Table 4). Lignin decay and enhanced oxidative enzyme activity have been shown to co-

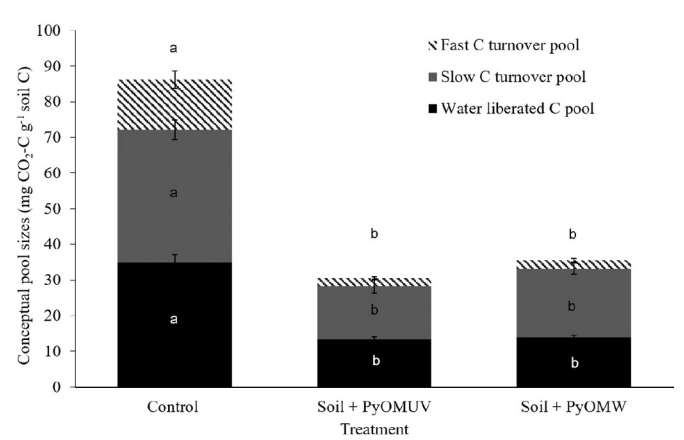


Fig. 2. The fast and slow native soil C (NSC) turnover pools, calculated from CO₂ liberated during the first 16 d of the incubation, and water liberated NSC pools, calculated from CO₂ liberated after soil rewetting on day 24, of unamended soil and soil amended with either photochemically weathered pyrogenic organic matter (PyOMUV) or control PyOM (PyOMW) treatments. Photochemical weathering was simulated by mixing PyOM for 4 weeks in a water slurry while exposed to UV-light (PyOMUV) and compared to PyOM mixed in a water slurry shielded from light as a dark control. Letters indicate significant differences among treatments ($\alpha=0.05$). Data represent means \pm standard error (n=5).

Table 4 Apparent phenol oxidase and peroxidase activities (μ mol g $^{-1}$ soil C) from 30 d incubations of unamended soil and soil amended with either photochemically weathered pyrogenic organic matter (PyOMUV) or control PyOM (PyOMW) treatments. Photochemical weathering was simulated by mixing PyOM for 4 weeks in a water slurry while exposed to UV-light (PyOMUV) and compared to PyOM mixed in a water slurry shielded from light as a dark control. Data represent means \pm standard error, n=5. Letters indicate significant differences among treatments ($\alpha=0.05$).

Treatments	Phenol oxidase activity (μ mol g ⁻¹ soil C)	Peroxidase activity (μ mol g ⁻¹ soil C)
Unamended soil	$15.1 \pm 0.42a$	57.9 ± 0.53a
Soil + PyOMUV	$26.6 \pm 0.28b$	60.6 ± 0.42b
Soil + PyOMW	$30.4 \pm 0.39c$	66.3 ± 0.40c

vary in soils (Robertson et al., 2008). If a selective positive priming effect related to lignin occurred in the present study one would expect greater $Ad/Al_{(S,V)}$ ratios, an indicator of lignin decomposition (Hedges et al., 1988; Kiem and Kögel-Knabner, 2003) to be evident. However, no change in these lignin proxies was observed in the present study. Alternatively, if the microbial decay mechanisms involved a brown rot or soft rot type of lignin decay there would be negligible increase in the $Ad/Al_{(S,V)}$ ratios generated by the CuO method (Filley et al., 2000; Filley et al., 2002). It is also feasible that the minor reduction in extractable lignin with added PyOM is the result of selective binding and protection of labile lignin to the surface of PyOM lowering the efficiency of the alkaline CuO oxidation procedure. Similar binding and selective molecular protection have been observed in soils containing metal hydroxyl oxides (Hernes et al., 2013) and is consistent with our interpretation of the large, negative PE for NSC observed after water addition at day 24.

4.3. Photochemical weathering of PyOM suppresses apparent soil oxidative enzymatic response

Although addition of both forms of PyOM caused an increased response in soil oxidative enzymes above the control soil, as we initially predicted, enzyme activities in the presence of PyOMUV were suppressed relative to PyOMW (Table 4). It is not surprising that the addition of PyOM would result in changes in enzyme activity relative to control treatments as previous studies have demonstrated both decreases and increases in microbial enzyme response with PyOM addition (Maestrini et al., 2015, Thies et al., 2015; Wang et al., 2016). We postulate that the relatively higher apparent phenol oxidase and peroxidase activity in the PyOMW treatment could have resulted from an upregulation in enzyme production by the soil microbes because of the greater availability of labile C in PyOMW compared with PyOMUV (Gibson et al., 2016). This is supported in part by the large pulse of ¹³CO₂ respired at the beginning of incubation in the PyOMW treatment though this pool is relatively small in comparison to the NSC labile C pool. The suppressed enzyme activity in the PyOMUV treatment can be explained by stronger surface binding, as was evident in the observed negative change in PE (Fig. 1). Such an enhanced chemisorption suppression of soil enzyme activity is consistent with recent observations of soil enzyme activities in the presence of PyOM (Cheng et al., 2006; Hilscher et al., 2009; Masiello et al., 2013). These findings are also consistent with previous studies that concluded distinct surface characteristics of PyOM induced by the aging or weathering process can increase surface binding of organics and reduce oxidative enzyme response (Wang et al., 2016; Zhao et al., 2015). While sorption has been proposed as the major mechanism for the difference in enzyme activities between fresh and aged PyOM in the study by Wang et al. (2016), water availability and growth in microbial biomass in aged PyOM treatments were also suggested as mechanisms for increased enzyme production in these treatments. This is also a possibility in the present study. An indication of the importance of surface binding on the two PyOM forms comes from the decreased respiration rates after water addition to the PyOM treatments (Fig. 2; Table 1) where we propose that irreversible binding of labile DOM or other key enzymes minimizes soil microbe accessibility to C with respect to control soils.

5. Conclusions

Our study sought to determine the effect of PyOM photochemical weathering on PyOM-C mineralization, NSC mineralization, oxidative enzyme activities, and the abundance of specific plant-derived biopolymers in the soil. The use of a ¹³C-labeled PyOM allowed us to distinguish mineralization of SOC from PyOM-C and assess SOC PE in this 30-day soil incubation experiment. While PyOM C mineralization was measured for both the photochemically weathered (PyOMUV) and the dark control PyOMW, the MRT and amount of labile PyOMUV-C mineralized was significantly less than that of PyOMW. Photochemical weathering of PyOM did not, however, result in a different NSC mineralization rate as both forms of PyOM promoted a reduction, i.e. negative priming, of approximately 50% relative to the unamended control soil. At the termination of the experiment, soil phenol oxidase enzyme activity and peroxidase activity increased with addition of both PyOMW and PyOMUV, by up to 200% for phenol oxidase with respect to unamended control soils. However, photochemical weathering resulted in approximately 10% lower enzyme activities compared to PyOMW. Our results indicate that PyOM photochemical weathering can impart important changes to short-term PyOM reactivity and soil microbial activity, which could have important implications for soil systems by ultimately lowering turnover rates for both NSC and PyOM-C.

Supplementary data to this article can be found online at http://dx.doi.org/10.1016/j.geoderma.2017.01.011.

Acknowledgments

The authors wish to acknowledge financial support from the National Science Foundation (BIO-1127253), the National Science Foundation of China (41301325), and U.S.-China Ecopartnership for Environmental Sustainability.

References

Almendros, G., González-Vila, F.J., Martín, F., Fründ, R., Lüdemann, H.-D., 1992. Advances in humic substances research solid state NMR studies of fire-induced changes in the structure of humic substances. Sci. Total Environ. 117:63–74. http://dx.doi.org/ 10.1016/0048-9697(92)90073-2.

Antiñolo, M., Willis, M.D., Zhou, S., Abbatt, J.P.D., 2015. Connecting the oxidation of soot to its redox cycling abilities. Nat. Commun. 6:6812. http://dx.doi.org/10.1038/ ncomms/812

Berry, T.D., Filley, T.R., Blanchette, R.A., 2014. Oxidative enzymatic response of white-rot fungi to single-walled carbon nanotubes. Environ. Pollut. 193:197–204. http://dx.doi.org/10.1016/j.envpol.2014.06.013.

Berry, T.D., Clavijo, A.P., Zhao, Y., Jafvert, C.T., Turco, R.F., Filley, T.R., 2016a. Soil microbial response to photo-degraded C60 fullerenes. Environ. Pollut. 211:338–345. http://dx.doi.org/10.1016/j.envpol.2015.12.025.

Berry, T.D., Filley, T.R., Clavijo, A.P., Bischoff Gray, M., Turco, R.F., 2016b. Degradation and microbial uptake of C60 fullerols in contrasting agricultural soils. Environ. Sci. Technol

Bird, J.A., Torn, M.S., 2006. Fine roots vs. needles: a comparison of 13C and 15 N dynamics in a ponderosa pine Forest soil. Biogeochemistry 79:361–382. http://dx.doi.org/10. 1007/s10533-005-5632-y.

Bond, T.C., Doherty, S.J., Fahey, D.W., Forster, P.M., Berntsen, T., DeAngelo, B.J., Flanner, M.G., Ghan, S., Kärcher, B., Koch, D., et al., 2013. Bounding the role of black carbon in the climate system: a scientific assessment. J. Geophys. Res.-Atmos. 118: 5380–5552. http://dx.doi.org/10.1002/jgrd.50171.2013.

Boonchan, S., Britz, M.L., Stanley, G.A., 2000. Degradation and mineralization of high-molecular-weight polycyclic aromatic hydrocarbons by defined fungal-bacterial co-cultures. Appl. Environ. Microbiol. 66:1007–1019. http://dx.doi.org/10.1128/AEM. 66:3.1007-1019.2000.

Borken, W., Matzner, E., 2009. Reappraisal of drying and wetting effects on C and N mineralization and fluxes in soils. Glob. Chang. Biol. 15:808–824. http://dx.doi.org/10. 1111/j.1365-2486.2008.01681.x.

Bouchez, M., Blanchet, D., Bardin, V., Haeseler, F., Vandecasteele, J.-P., 1999. Efficiency of defined strains and of soil consortia in the biodegradation of polycyclic aromatic hydrocarbon (PAH) mixtures. Biodegradation 10:429–435. http://dx.doi.org/10.1023/A: 1008382030604.

Brodowski, S., Rodionov, A., Haumaier, L., Glaser, B., Amelung, W., 2005. Revised black carbon assessment using benzene polycarboxylic acids. Org. Geochem. 36:1299–1310. http://dx.doi.org/10.1016/j.orggeochem.2005.03.011.

- Bruun, E.W., Hauggaard-Nielsen, H., Ibrahim, N., Egsgaard, H., Ambus, P., Iensen, P.A., Dam-Johansen, K., 2011. Influence of fast pyrolysis temperature on biochar labile fraction and short-term carbon loss in a loamy soil. Biomass Bioenergy 35: 1182-1189. http://dx.doi.org/10.1016/i.biombioe.2010.12.008.
- Chatterjee, S., Santos, F., Abiven, S., Itin, B., Stark, R.E., Bird, J.A., 2012. Elucidating the chemical structure of pyrogenic organic matter by combining magnetic resonance, mid-infrared spectroscopy and mass spectrometry. Org. Geochem. 51:35-44. http:// dx.doi.org/10.1016/j.orggeochem.2012.07.006.
- Cheng, C.-H., Lehmannn, J., Thies, J.E., Burton, S.D., Engelhard, M.H., 2006. Oxidation of black carbon by biotic and abiotic processes. Org. Geochem. 37:14771488. http:// dx.doi.org/10.1016/j.orggeochem.2006.06.022.
- Cheng, C.-H., Lehmannn, J., Engelhard, M.H., 2008. Natural oxidation of black carbon in soils: changes in molecular form and surface charge along a climosequence. Geochim. Cosmochim. Acta 72:1598-1610. http://dx.doi.org/10.1016/j.gca.2008.01.010.
- Cong, Z., Kang, S., Gao, S., Zhang, Y., Li, Q., Kawamura, K., 2013. Historical trends of atmospheric black carbon on Tibetan plateau as reconstructed from a 150-year Lake sediment record. Environ. Sci. Technol. 47:2579-2586. http://dx.doi.org/10.1021/ es3048202
- Creamer, C.A., Filley, T.R., Boutton, T.W., Oleynik, S., Kantola, I.B., 2011. Controls on soil carbon accumulation during woody plant encroachment: evidence from physical fractionation, soil respiration, and δ^{13} C of respired CO₂. Soil Biol. Biochem. 43: 1678-1687. http://dx.doi.org/10.1016/j.soilbio.2011.04.013.
- Czimczik, C.I., Schmidt, M.W.I., Schulze, E.-D., 2005. Effects of increasing fire frequency on black carbon and organic matter in Podzols of Siberian Scots pine forests, Eur. J. Soil Sci. 56:417-428. http://dx.doi.org/10.1111/j.1365-2389.2004.00665.x.
- Fierer, N., Schimel, J.P., 2002. Effects of drying-rewetting frequency on soil carbon and ni-
- trogen transformations. Soil Biol. Biochem. 34, 777–787. Filley, T.R., Hatcher, P.G., Shortle, W.C., Praseuth, R.T., 2000. The application of ¹³C-labeled tetramethylammonium hydroxide (13 C-TMAH) thermochemolysis to the study of fungal degradation of wood. Org. Geochem. 31:181-198. http://dx.doi.org/10.1016/ S0146-6380(99)00159-X.
- Filley, T.R., Cody, G.D., Goodell, B., Jellison, J., Noser, C., Ostrofsky, A., 2002. Lignin demethylation and polysaccharide decomposition in spruce sapwood degraded by brown rot fungi. Org. Geochem. 33:111-124. http://dx.doi.org/10.1016/S0146-6380(01)00144-
- Filley, T.R., Boutton, T.W., Liao, J.D., Jastrow, J.D., Gamblin, D.E., 2008. Chemical changes to nonaggregated particulate soil organic matter following grassland-to-woodland transition in a subtropical savanna. J. Geophys. Res. Biogeosci. 113, G03009. http://dx.doi. org/10.1029/2007JG000564.
- Gibson, C., Berry, T.D., Wang, R., Spencer, J.A., Johnston, C.T., Jiang, Y., Bird, J.A., Filley, T.R., 2016. Weathering of pyrogenic organic matter induces fungal oxidative enzyme response in single culture inoculation experiments. Org. Geochem. 92:32-41. http:// dx.doi.org/10.1016/j.orggeochem.2015.12.003.
- Glaser, B., Haumaier, L., Guggenberger, G., Zech, W., 1998. Black carbon in soils: the use of benzenecarboxylic acids as specific markers. Org. Geochem. 29:811-819. http://dx. doi.org/10.1016/S0146-6380(98)00194-6
- Glaser, B., Guggenberger, G., Zech, W., 2001. Black carbon in sustainable soils of the Brazilian Amazon region. Underst. Manag. Org. Matter Soils Sediments Waters Int. Humic Subst. Soc. St Paul MN, pp. 359-364.
- Goñi, M.A., Hedges, J.I., 1990. Potential applications of cutin-derived CuO reaction products for discriminating vascular plant sources in natural environments. Geochim. Cosmochim. Acta 54:3073-3081. http://dx.doi.org/10.1016/0016-7037(90)90123-3.
- Hamilton, G.A., Hartnett, H.E., 2013. Soot black carbon concentration and isotopic composition in soils from an arid urban ecosystem. Org. Geochem. 59:87-94. http://dx.doi. org/10.1016/j.orggeochem.2013.04.003.
- Hammes, K., Smernik, R.J., Skjemstad, J.O., Herzog, A., Vogt, U.F., Schmidt, M.W., 2006. Synthesis and characterisation of laboratory-charred grass straw (Oryza sativa) and chestnut wood (Castanea sativa) as reference materials for black carbon quantification. Org. Geochem. 37:1629-1633. http://dx.doi.org/10.1016/j.orggeochem.2006.
- Hatton, P.-J., Chatterjee, S., Filley, T.R., Dastmalchi, K., Plante, A.F., Abiven, S., Gao, X., Masiello, C.A., Leavitt, S.W., Nadelhoffer, K.J., Stark, R.E., Bird, J.A., 2016. Tree taxa and pyrolysis temperature interact to control the efficacy of pyrogenic organic matter formation. Biogeochemistry 130:103-116. http://dx.doi.org/10.1007/s10533-016-
- Hedges, J.I., Ertel, J.R., Leopold, E.B., 1982. Lignin geochemistry of a late quaternary sediment core from Lake Washington. Geochim. Cosmochim. Acta 46:1869-1877. http://dx.doi.org/10.1016/0016-7037(82)90125-9.
- Hedges, J.I., Blanchette, R.A., Weliky, K., Devol, A.H., 1988. Effects of fungal degradation on the CuO oxidation products of lignin: a controlled laboratory study. Geochim. Cosmochim. Acta 52:2717-2726. http://dx.doi.org/10.1016/0016-7037(88)90040-3.
- Hernes, P.J., Kaiser, K., Dyda, R.Y., Cerli, C., 2013. Molecular trickery in soil organic matter: hidden lignin. Environ. Sci. Technol. 47:9077-9085. http://dx.doi.org/10.1021/ es401019n.
- Hilscher, A., Heister, K., Siewert, C., Knicker, H., 2009. Mineralisation and structural changes during the initial phase of microbial degradation of pyrogenic plant residues in soil. Org. Geochem. 40:332–342. http://dx.doi.org/10.1016/j.orggeochem.2008.12.004.
- Hockaday, W.C., Grannas, A.M., Kim, S., Hatcher, P.G., 2006. Direct molecular evidence for the degradation and mobility of black carbon in soils from ultrahighresolution mass spectral analysis of dissolved organic matter from a fire-impacted forest soil. Org. Geochem. 37:501-510. http://dx.doi.org/10.1016/j.orggeochem. 2005.11.003.
- Jaffé, R., Ding, Y., Niggemann, J., Vähätalo, A.V., Stubbins, A., Spencer, R.G., Campbell, J., Dittmar, T., 2013. Global charcoal mobilization from soils via dissolution and riverine

- transport to the oceans. Science 340:345–347. http://dx.doi.org/10.1126/science. 1231476
- Jain, S., Mishra, D., Khare, P., Yadav, V., Deshmukh, Y., Meena, A., 2016. Impact of biochar amendment on enzymatic resilience properties of mine spoils. Sci. Total Environ. 544:410–421. http://dx.doi.org/10.1016/i.scitotenv.2015.11.011.
- Jin, Y., Liang, X., He, M., Liu, Y., Tian, G., Shi, J., 2016. Manure biochar influence upon soil properties, phosphorus distribution and phosphatase activities: A microcosm incubation study. Chemosphere 142:128–135. http://dx.doi.org/10.1016/j.chemosphere. 2015 07 015
- Kasozi, G.N., Zimmerman, A.R., Nkedi-Kizza, P., Gao, B., 2010. Catechol and humic acid sorption onto a range of laboratory-produced black carbons (biochars). Environ. Sci. Technol. 44:6189-6195. http://dx.doi.org/10.1021/es1014423.
- Keiluweit, M., Nico, P.S., Johnson, M.G., Kleber, M., 2010. Dynamic molecular structure of plant biomass-derived black carbon (biochar), Environ, Sci. Technol, 44, 1247–1253.
- Kiem, R., Kögel-Knabner, I., 2003. Contribution of lignin and polysaccharides to the refractory carbon pool in C-depleted arable soils. Soil Biol. Biochem. 35:101–118. http://dx. doi.org/10.1016/S0038-0717(02)00242-0.
- Kim, K.H., Jeong, H.S., Kim, J.-Y., Han, G.S., Choi, I.-G., Choi, J.W., 2012. Evaluation of the antifungal effects of bio-oil prepared with lignocellulosic biomass using fast pyrolysis technology. Chemosphere 89:688–693. http://dx.doi.org/10.1016/j.chemosphere. 2012 06 010
- Kuzyakov, Y., Subbotina, I., Chen, H., Bogomolova, I., Xu, X., 2009. Black carbon decomposition and incorporation into soil microbial biomass estimated by ¹⁴C labeling. Soil Biol. Biochem. 41:210-219. http://dx.doi.org/10.1016/j.soilbio.2008.10.016.
- Kuzyakov, Y., Bogomolova, I., Glaser, B., 2014. Biochar stability in soil: Decomposition during eight years and transformation as assessed by compound-specific ¹⁴C analysis. Soil Biol. Biochem. 70:229-236. http://dx.doi.org/10.1016/j.soilbio.2013.12.021.
- Laird, D., Fleming, P., Wang, B., Horton, R., Karlen, D., 2010. Biochar impact on nutrient leaching from a Midwestern agricultural soil. Geoderma 158, 436-442.
- Lammirato, C., et al., 2011. Hydrolysis of Cellobiose by β-Glucosidase from Aspergillus Niger in the Presence of Soil Solid Phases: Minerals, Biochar, and Activated Carbon. Technische Universität München.
- LeCroy, C., Masiello, C.A., Rudgers, J.A., Hockaday, W.C., Silberg, J.J., 2013. Nitrogen, biochar, and mycorrhizae: Alteration of the symbiosis and oxidation of the char surface. Soil Biol. Biochem. 58:248-254. http://dx.doi.org/10.1016/j.soilbio.2012.11.023.
- Lehmann, J., Rillig, M.C., Thies, J., Masiello, C.A., Hockaday, W.C., Crowley, D., 2011. Biochar effects on soil biota-a review. Soil Biol. Biochem. 43:1812-1836. http://dx.doi.org/10. 1016/j.soilbio.2011.04.022.
- Lehmann, J., Abiven, S., Kleber, M., Pan, G., Singh, B.P., Sohi, S.P., Zimmerman, A.R., Lehmann, J., Joseph, S., 2015. Persistence of biochar in soil. Biochar Environ. Manag. Sci. Technol. Implement, pp. 233–280.
- Lin, X.W., Xie, Z.B., Zheng, J.Y., Liu, Q., Bei, Q.C., Zhu, J.G., 2015. Effects of biochar application on greenhouse gas emissions, carbon sequestration and crop growth in coastal saline soil. Eur. J. Soil Sci. 66:329–338. http://dx.doi.org/10.1111/ejss.12225.
- Liu, Z., Demisie, W., Zhang, M., 2013. Simulated degradation of biochar and its potential environmental implications. Environ. Pollut. 179:146-152. http://dx.doi.org/10. 1016/j.envpol.2013.04.030.
- Luo, Y., Durenkamp, M., De Nobili, M., Lin, Q., Brookes, P.C., 2011. Short term soil priming effects and the mineralisation of biochar following its incorporation to soils of different pH. Soil Biol. Biochem. 43:2304-2314. http://dx.doi.org/10.1016/j.soilbio.2011.07.
- Maestrini, B., Herrmann, A.M., Nannipieri, P., Schmidt, M.W.I., Abiven, S., 2014. Ryegrassderived pyrogenic organic matter changes organic carbon and nitrogen mineralization in a temperate forest soil. Soil Biol. Biochem. 69:291-301. http://dx.doi.org/10. 1016/j.soilbio.2013.11.013.
- Maestrini, B., Nannipieri, P., Abiven, S., 2015. A meta-analysis on pyrogenic organic matter induced priming effect. GCB Bioenergy 7:577-590. http://dx.doi.org/10.1111/gcbb.
- Mannino, A., Harvey, H.R., 2004. Black carbon in estuarine and coastal ocean dissolved organic matter. Limnol. Oceanogr. 49, 735-740.
- Masiello, C.A., Druffel, E.R.M., 1998. Black carbon in deep-sea sediments. Science 280: 1911-1913. http://dx.doi.org/10.1126/science.280.5371.1911.
- Masiello, C.A., Chen, Y., Gao, X., Liu, S., Cheng, H.-Y., Bennett, M.R., Rudgers, J.A., Wagner, D.S., Zygourakis, K., Silberg, J.J., 2013. Biochar and microbial signaling: production conditions determine effects on microbial communication. Environ. Sci. Technol. 47:11496-11503. http://dx.doi.org/10.1021/es401458s.
- McFarlane, K.J., Torn, M.S., Hanson, P.J., Porras, R.C., Swanston, C.W., Callaham Jr., M.A., Guilderson, T.P., 2012. Comparison of soil organic matter dynamics at five temperate deciduous forests with physical fractionation and radiocarbon measurements. Biogeochemistry 112:457-476. http://dx.doi.org/10.1007/s10533-012-9740-1.
- McKenna, E., Andreas, A., 1997. South Park Mountain Data: South Park, Colorado (data) (No. NREL Report No. DA-5500-56521).
- Middelburg, J.J., Nieuwenhuize, J., van Breugel, P., 1999. Black carbon in marine sediments. Mar. Chem. 65:245-252. http://dx.doi.org/10.1016/S0304-4203(99)00005-5.
- Mikha, M.M., Rice, C.W., Milliken, G.A., 2005. Carbon and nitrogen mineralization as affected by drying and wetting cycles. Soil Biol. Biochem. 37:339-347. http://dx.doi. org/10.1016/j.soilbio.2004.08.003.
- Murray, J., Keith, A., Singh, B., 2015. The stability of low-and high-ash biochars in acidic soils of contrasting mineralogy. Soil Biol. Biochem. 89:217-225. http://dx.doi.org/ 10.1016/j.soilbio.2015.07.014.
- Navarro-García, F., Casermeiro, M.Á., Schimel, J.P., 2012. When structure means conservation: Effect of aggregate structure in controlling microbial responses to rewetting events, Soil Biol, Biochem. 44:1–8. http://dx.doi.org/10.1016/j.soilbio.2011.09.019.
- Nguyen, B.T., Lehmannn, J., Kinyangi, J., Smernik, R., Riha, S.J., Engelhard, M.H., 2009. Longterm black carbon dynamics in cultivated soil. Biogeochemistry 92:163-176. http:// dx.doi.org/10.1007/s10533-008-9248-x.

- Paul, E.A., Morris, S.J., Bohm, S., 2001. The determination of soil C pool sizes and turnover rates; biophysical fractionation and tracers. Assess, Methods Soil Carbon 14, 193–206.
- Peng, R.-H., Xiong, A.-S., Xue, Y., Fu, X.-Y., Gao, F., Zhao, W., Tian, Y.-S., Yao, Q.-H., 2008. Microbial biodegradation of polyaromatic hydrocarbons. FEMS Microbiol. Rev. 32: 927–955. http://dx.doi.org/10.1111/j.1574-6976.2008.00127.x.
- Prendergast-Miller, M.T., Duvall, M., Sohi, S.P., 2014. Biochar-root interactions are mediated by biochar nutrient content and impacts on soil nutrient availability. Eur. J. Soil Sci. 65:173–185. http://dx.doi.org/10.1111/eiss.12079.
- Robertson, S.A., Mason, S.L., Hack, E., Abbott, G.D., 2008. A comparison of lignin oxidation, enzymatic activity and fungal growth during white-rot decay of wheat straw. Org. Geochem. 39, 945–951.
- Ryan, K.C., 2002. Dynamic interactions between forest structure and fire behavior in boreal ecosystems. Silva Fenn. 36, 13–39.
- Santín, C., Doerr, S.H., Preston, C.M., González-Rodríguez, G., 2015. Pyrogenic organic matter production from wildfires: a missing sink in the global carbon cycle. Glob. Chang. Biol. 21:1621–1633. http://dx.doi.org/10.1111/gcb.12800.
- Santín, C., Doerr, S.H., Merino, A., Bryant, R., Loader, N.J., 2016. Forest floor chemical transformations in a boreal forest fire and their correlations with temperature and heating duration. Geoderma 264:71–80. http://dx.doi.org/10.1016/j.geoderma.2015.09.021.
- Santos, F., Torn, M.S., Bird, J.A., 2012. Biological degradation of pyrogenic organic matter in temperate forest soils. Soil Biol. Biochem. 51:115–124. http://dx.doi.org/10.1016/j. soilbio.2012.04.005.
- Schmidt, M.W., Skjemstad, J.O., Czimczik, C.I., Glaser, B., Prentice, K.M., Gelinas, Y., Kuhlbusch, T.A., 2001. Comparative analysis of black carbon in soils. Glob. Biogeochem. Cycles 15, 163–167 (doi:2000GB001284).
- Schreiner, K.M., Filley, T.R., Blanchette, R.A., Bowen, B.B., Bolskar, R.D., Hockaday, W.C., Masiello, C.A., Raebiger, J.W., 2009. White-rot Basidiomycete-mediated decomposition of C60 Fullerol. Environ. Sci. Technol. 43:3162–3168. http://dx.doi.org/10.1021/ es801873a.
- Singh, B.P., Cowie, A.L., 2014. Long-term influence of biochar on native organic carbon mineralisation in a low-carbon clayey soil. Sci. Rep. 4. http://dx.doi.org/10.1038/srap03687
- Singh, N., Abiven, S., Torn, M.S., Schmidt, M.W.I., 2012. Fire-derived organic carbon in soil turns over on a centennial scale. Biogeosciences 9:2847–2857. http://dx.doi.org/10. 5194/bg-9-2847-2012.

- Skjemstad, J.O., Reicosky, D.C., Wilts, A.R., McGowan, J.A., 2002. Charcoal carbon in US agricultural soils. Soil Sci. Soc. Am. J. 66:1249–1255. http://dx.doi.org/10.2136/sssai2002.1249.
- Smernik, R., Skjemstad, J., 2008. Mechanisms of organic matter stabilization and destabilization in soils and sediments: conference introduction. Biogeochemistry 92:3–8. http://dx.doi.org/10.1007/s10533-008-9269-5.
- Thies, J.E., Rillig, M.C., Graber, E.R., 2015. Biochar effects on the abundance, activity and diversity of the soil biota. Biochar Environ. Manag. Sci. Technol. Earthscan Books Ltd Lond, pp. 327–389.
- van Lierop, W., 1990. Soil pH and Lime Requirement Determination. Soil Science Society of America, pp. 73–126.
- Wang, J., Dokohely, M.E., Xiong, Z., Kuzyakov, Y., 2016. Contrasting effects of aged and fresh biochars on glucose-induced priming and microbial activities in paddy soil. I. Soils Sediments 16:191–203. http://dx.doi.org/10.1007/s11368-015-1189-0.
- Weintraub, M.N., Scott-Denton, L.E., Schmidt, S.K., Monson, R.K., 2007. The effects of tree rhizodeposition on soil exoenzyme activity, dissolved organic carbon, and nutrient availability in a subalpine forest ecosystem. Oecologia 154:327–338. http://dx.doi. org/10.1007/s00442-007-0804-1.
- Yarnes, C., Santos, F., Singh, N., Abiven, S., Schmidt, M.W., Bird, J.A., 2011. Stable isotopic analysis of pyrogenic organic matter in soils by liquid chromatography–isotoperatio mass spectrometry of benzene polycarboxylic acids. Rapid Commun. Mass Spectrom. 25:3723–3731. http://dx.doi.org/10.1002/rcm.5272.
- Yao, Y., Gao, B., Zhang, M., Inyang, M., Zimmerman, A.R., 2012. Effect of biochar amendment on sorption and leaching of nitrate, ammonium, and phosphate in a sandy soil. Chemosphere 89, 1467–1471.
- Zhao, R., Coles, N., Wu, J., 2015. Carbon mineralization following additions of fresh and aged biochar to an infertile soil. Catena 125:183–189. http://dx.doi.org/10.1016/j.catena 2014 10 026
- Zimmerman, A.R., 2010. Abiotic and microbial oxidation of laboratory-produced black carbon (biochar). Environ. Sci. Technol. 44:1295–1301. http://dx.doi.org/10.1021/es903140c.
- Zimmerman, A.R., Gao, B., Ahn, M.-Y., 2011. Positive and negative carbon mineralization priming effects among a variety of biochar-amended soils. Soil Biol. Biochem. 43: 1169–1179. http://dx.doi.org/10.1016/j.soilbio.2011.02.005.